

Research Regarding Molybdenum Flakes' Improvement on the Hydrogen Storage Efficiency of MgH₂

Changshan Cheng, Haoyu Zhang, Mengchen Song, Fuying Wu * and Liuting Zhang *

School of Energy and Power, Instrumental Analysis Center, Jiangsu University of Science and Technology, Zhenjiang 212003, China; 209210043@stu.just.edu.cn (C.C.); 202210009@stu.just.edu.cn (H.Z.); 202210007@stu.just.edu.cn (M.S.)

* Correspondence: wufuying@just.edu.cn (F.W.); zhanglt89@just.edu.cn (L.Z.);
Tel.: +86-18344819581 (F.W.); +86-15262913186 (L.Z.)

Abstract: As an efficient hydrogen storage material, magnesium hydride (MgH₂) has a high capacity of 7.6 wt%. However, its performance deteriorates because of high thermodynamic and kinetic temperatures and the fast agglomeration of its nanocrystals during the hydrogen uptake and release process. The exploration of efficient catalysts is a popular, but currently challenging, topic. Therefore, we successfully prepared flake-like molybdenum (Mo) catalysts and doped them into MgH₂ to enhance its properties. We found that the incorporation of 7wt%Mo into MgH₂ could reduce the starting desorption temperature by approximately 100 °C. In addition, the 7wt%Mo-doped MgH₂ could desorb almost all of the H₂ within 20 min at a 325 °C isothermal condition. For hydrogenation, MgH₂-7wt%Mo could absorb approximately 5 wt% of hydrogen within 5 min at a 250 °C isothermal condition with a hydrogen pressure of 3 MPa. In addition, the MgH₂-7wt%Mo composite could maintain approximately 98% of the initial capacity at the end of 22 cycles, presenting good cycling performance.

Keywords: hydrogen storage; magnesium hydride; molybdenum flakes; catalysis



Citation: Cheng, C.; Zhang, H.; Song, M.; Wu, F.; Zhang, L. Research Regarding Molybdenum Flakes' Improvement on the Hydrogen Storage Efficiency of MgH₂. *Metals* **2023**, *13*, 631. <https://doi.org/10.3390/met13030631>

Academic Editor: Tomasz Czujko

Received: 1 March 2023

Revised: 18 March 2023

Accepted: 20 March 2023

Published: 22 March 2023



Copyright: © 2023 by the authors. Licensee MDPI, Basel, Switzerland. This article is an open access article distributed under the terms and conditions of the Creative Commons Attribution (CC BY) license (<https://creativecommons.org/licenses/by/4.0/>).

1. Introduction

Hydrogen energy is regarded as one of the best energy sources to achieve carbon neutrality, as it has a high energy density, is non-toxic and environmentally protective, and has zero emissions. According to a report by the International Energy Agency (IEA), hydrogen could provide up to 18% of the world's total energy needs by 2050 [1–3]. The development and application of hydrogen energy are still hindered by the lack of high-capacity and safe hydrogen storage technology [3–6]. Compared with high-pressure gaseous hydrogen storage (35–70 MPa at room temperature) and low-temperature liquid hydrogen storage (−253 °C, 0.5–1 MPa), solid-state hydrogen storage has some advantages in terms of transportation, storage, and safety [7–9].

Among the various solid-state hydrogen storage materials, magnesium hydride (MgH₂) has been widely investigated for its high capacity (110 g/L) and weight (7.6 wt%) content, abundant magnesium element, and low cost [10–15]. To overcome the problems of slow hydrogen uptake and dehydrogenation, high desorption temperature (>350 °C), and weak cycling performance of MgH₂, strategies including surface modification, combination with other hydrides, nanostructuring, and catalyst doping have been tested to improve its performance. Daniel Fruchart et al. used the HPT (High-pressure Torsion) technique for the first time to successfully consolidate metal hydride powders (MgH₂). When MgH₂ was used instead of Mg as a raw material, a very significant grain refinement was achieved, resulting in an average size range of 10–30 nm [16]. Catalyst doping is considered one of the most feasible modification strategies, which contributes significantly to promoting the improvement of the de/hydrogenation performance of MgH₂ [17–28].

Among the catalysts that have been developed so far, transition metal catalysts have been found to have considerable catalytic activity, including Mn, Co, Ti, Nb, V, and Mo,

and their compounds [29–34]. For example, Jacques Huot et al. found that the hydrogen storage properties of MgH_2 were significantly improved by nanostructuring and adding crystals such as Nb and V [35]. Chen et al. [36] reported that Mn nanoparticles doped using MgH_2 could start hydrogen absorption at room temperature with a hydrogen absorption content of 2.0 wt% within 30 min at a low temperature of 50 °C. Jia et al. [37] investigated the catalytic effect of MoS_2 and MoO_2 on the hydrogen adsorption/desorption kinetics of MgH_2 ; the enhanced hydrogenation/dehydrogenation kinetics of MgH_2 were due to the presence of MgS and Mo. Chen et al. [38] found that MoNi alloys could promote breaking the Mg-H bond and thus improve the kinetics of the Mg/ MgH_2 system. At 300 °C, MoNi-catalyzed Mg/ MgH_2 could absorb 6.7 wt% of hydrogen in 60 s and released 6.7 wt% of hydrogen in 10 min at the same temperature. Xia et al. [39] found that Mo formed by the reaction of LiBH_4 and MoCl_3 plays an important role in improving the dehydrogenation and hydrogenation properties of the LiBH_4 - MgH_2 system.

We investigated the effect of molybdenum pentachloride on the performance of MgH_2 and found that the onset dehydrogenation temperature of molybdenum pentachloride-doped MgH_2 was approximately 295 °C. Wang et al. [40] investigated the structural and energetic properties of H, F, and Cl defects in MgH_2 using density flooding theory and supercell methods; they found that F and Cl do not reduce the removal energy of neutral and negatively charged H. There is also no previous study regarding the direct use of molybdenum to improve the hydrogen storage performance of MgH_2 . Therefore, we successfully prepared lamellar Mo via wet chemical ball milling and subsequently doped the catalyst into MgH_2 to enhance its hydrogen storage performance. Hydrogen storage performance tests showed that the onset dehydrogenation temperature of flake-like Mo-doped MgH_2 could be reduced to 250 °C, which is approximately 100 °C lower than that of pure MgH_2 . Combining hydrogen storage performance with microstructure analysis, the catalytic mechanism of lamellar Mo was further explored.

2. Experimental Section

2.1. Synthesis of MgH_2

Hydrogenation heat treatment and mechanical ball milling were used to prepare MgH_2 samples. In a nutshell, a volumetric Sieverts-type device hydrogenated the magnesium granules at 380 °C and 65 bar of hydrogen pressure. The samples were then put into a planetary ball mill system (QM-3SP4, Nanjing Chishun, Nanjing, China) at 450 rpm for 5 h with a 40:1 ball-to-powder ratio by weight. After repeating the aforementioned processes twice, MgH_2 was produced.

2.2. Synthesis of Flake-like Mo

Wet chemical ball milling was used to create Mo flakes with high purity. Initially, 0.1 mL of oleylamine, 0.3 mL of oleic acid, and 6 mL of n-heptane were added to 2 g of molybdenum powders (Alfa molybdenum powder, 250 mesh, 99.9% (metals basis)) in a ball mill jar. The mixture was then ball milled for 45 h. The liquid was transferred to a centrifuge tube following the ball-milling process. Anhydrous ethanol was adopted to wash the products. Finally, Mo flakes were produced by drying the material in a drying oven.

2.3. Preparation of MgH_2 - MoCl_5 and MgH_2 -Mo Composites

MgH_2 was combined with the purchased MoCl_5 (molybdenum (V) chloride, Adamas, 99.6% purity) particles and Mo flakes in a ball-mill tank. The combination was then processed for 2 h at 450 rpm/min, 1 MPa Ar pressure, and a 40:1 ball-to-powder ratio in a planetary ball mill. MgH_2 - $x\text{wt}\%\text{MoCl}_5$ (MgH_2 - $x\text{wt}\%\text{MoCl}_5$, $x = 3, 5, 7, 9$) and MgH_2 - $x\text{wt}\%\text{Mo}$ (MgH_2 - $x\text{wt}\%$, $x = 3, 5, 7, 9$) composites were produced. All samples were maintained in an argon-filled glove box with a water/oxygen level below 1 ppm before testing to prevent contamination from air and moisture.

2.4. Characterization

X-ray diffraction (XRD) was used to examine the materials' crystal structure using a Rigaku D/max 2500PC X-ray diffractometer with Cu K α radiation. The morphology of the samples was examined using TEM via a JEM-2100 JEOL tool. Using a pressure–composition–temperature instrument of the Sieverts type, the samples' capacity to store hydrogen was evaluated. Sample containers were filled with 200 mg of samples (in a glove box). All samples were heated to 450 °C at a heating rate of 2 °C per minute for isothermal desorption. At 380 °C and 3 MPa of initial hydrogen pressure, tests regarding the kinetics of rehydrogenation were conducted. The weight of the complete composite, including the catalyst, was noted, together with the hydrogen storage capacity as a percentage.

3. Results and Discussion

3.1. Characterization of As-Prepared Mo

Figure 1a provides the XRD pattern of the synthesized Mo. The diffraction peaks are well matched with the PDF card of Mo, and the three strong peaks correspond to the (110), (200), and (211) planes of Mo. The morphology of as-prepared Mo was investigated using transmission electron microscopy. Figure 1b shows that the as-prepared Mo was in the form of a flake structure. In particular, the high-resolution transmission electron microscopy results shown in Figure 1c indicate that the distance between the lattice stripes was 0.222 nm, which was in good agreement with the (110) lattice plane of Mo.

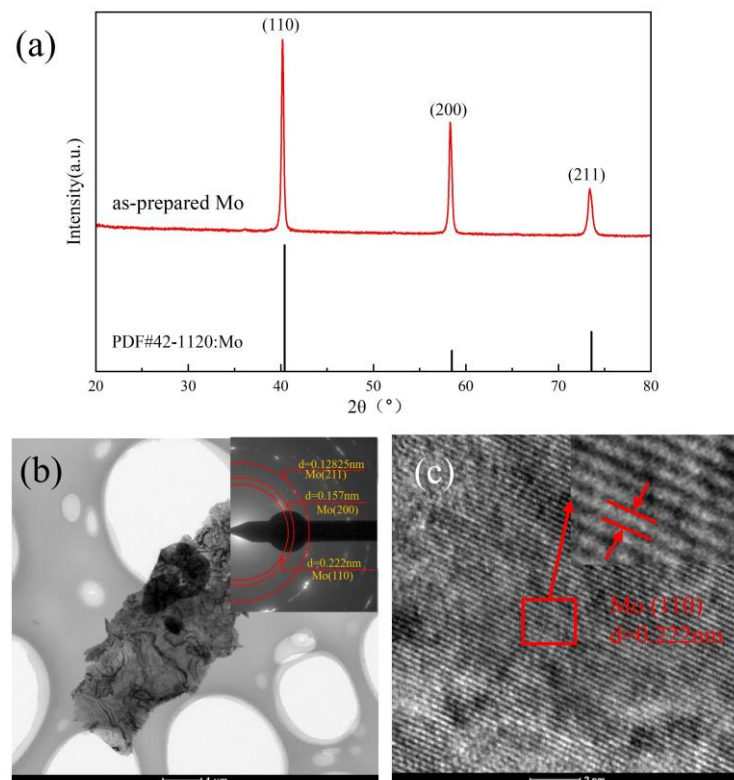


Figure 1. (a) XRD pattern, (b) TEM image, and (c) HRTEM image of as-prepared Mo. SAED pattern was also compiled in (b).

3.2. Catalytic Effect of Mo on the Hydrogen Storage Properties of MgH₂

In analyzing the effect of MoCl₅ and Mo on the hydrogen release performance of MgH₂, we found that pure Mo was more effective than MoCl₅ (Figure 2a). To uncover the best doping amount of Mo, non-isothermal hydrogen release curves of different MgH₂-Mo composites were compared. As shown in Figure 2b, MgH₂ exhibited the highest onset dehydrogenation temperature. The onset temperature of MgH₂-Mo composites was close to 270 °C. However, as the doping amount of Mo increased, the dehydrogenation

temperature of MgH₂ decreased, along with its capacity for dehydrogenation. Therefore, MgH₂-7wt%Mo was chosen as the optimal ratio for later study due to its large dehydrogenation capacity, even at a lower dehydrogenation temperature. As illustrated in Figure 2c, for MgH₂ without a catalyst, there was almost no dehydrogenation occurring at 300 °C for 60 min, and only approximately 7 wt% of hydrogen was released at 325 °C for 60 min. The dehydrogenation rate of the prepared MgH₂ significantly accelerated when the temperature was increased to 375 °C. Approximately 7.5 wt% of hydrogen could be dehydrogenated at 375 °C for 10 min. For the MgH₂-7wt%Mo composites (Figure 2d), all the hydrogen could be released at 325 °C and 350 °C in 25 min, and approximately 6.8 wt% hydrogen was desorbed in one hour at 300 °C. Approximately 2.0 wt% of hydrogen was released in one hour at the lowest test temperature of 275 °C.

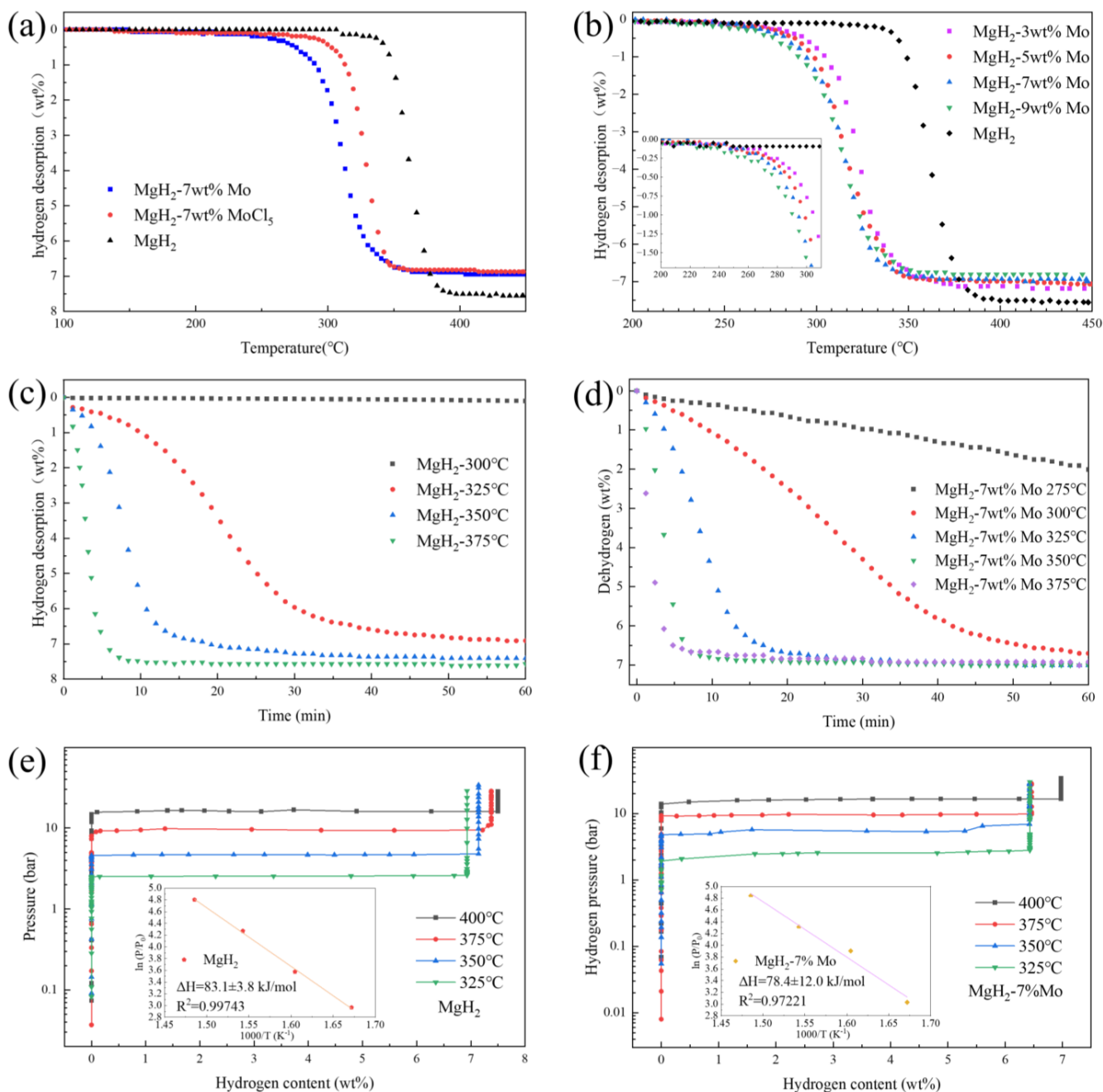


Figure 2. (a) Non-isothermal dehydrogenation curves of MgH₂, MgH₂-7wt%MoCl₅, and MgH₂-7wt%Mo; (b) non-isothermal dehydrogenation curves for MgH₂, MgH₂-3wt%Mo, MgH₂-5wt%Mo,

MgH₂-7wt%Mo, and MgH₂-9wt%Mo; (c) isothermal dehydrogenation curves of MgH₂ at 300, 325, 350, and 375 °C; (d) isothermal dehydrogenation curves of MgH₂-7wt%Mo at 275, 300, 325, and 350 °C; (e) pressure-composites-temperature (PCT) curves of MgH₂ at different temperatures, and corresponding van't Hoff plot; (f) pressure-composites-temperature (PCT) curves of MgH₂-7wt%Mo at different temperatures, and corresponding van't Hoff plot.

To further investigate the effect of Mo on the thermodynamic properties of MgH₂, the plateau hydrogen pressures of MgH₂ and MgH₂-7wt%Mo at different temperatures were determined. The plateau pressures for the desorption of MgH₂ at 325 °C, 350 °C, 375 °C, and 400 °C were 2.54, 4.68, 9.83, and 16.79 bar, respectively. Conversely, the plateau pressures for the MgH₂-7wt%Mo composite at the same temperatures were 2.7, 6.5, 10.64, and 17 bar, respectively. By calculating the corresponding enthalpies of hydrogen decomposition (ΔH), as shown in Figure 2e,f, it was determined that the enthalpy of the MgH₂ was 83.1 ± 3.8 kJ/mol, and that the enthalpy of the composite with the catalyst was 78.4 ± 12 kJ/mol, which is slightly lower than that of pure MgH₂. Therefore, the addition of flake-like Mo had a limited effect on the thermodynamic properties of magnesium hydride.

The effect of Mo on the hydrogen absorption performance of MgH₂ was investigated under isothermal/non-isothermal conditions at a hydrogen pressure of approximately 3 MPa. Figure 3a shows the non-isothermal hydrogen uptake curves under the same conditions, and it can be seen that MgH₂-7wt%Mo started to absorb hydrogen at 50 °C, whereas the prepared MgH₂ began to absorb hydrogen after 150 °C. As shown in Figure 3b, MgH₂-7wt%Mo adsorbed approximately 3 wt% of hydrogen in a period of 30 min under 175 °C, which is twice the hydrogen adsorption capacity of MgH₂ (1.5 wt%). As shown in Figure 3c, at an adsorption temperature of 225 °C, MgH₂-7wt%Mo was able to adsorb approximately 6 wt% of hydrogen in 30 min, whereas MgH₂ achieved less than 5.5 wt% of hydrogen at 30 min, and eventually approached saturation after 60 min. As shown in Figure 3d, when the adsorption temperature was set to 250 °C, MgH₂-7wt%Mo was close to saturation after 20 min, whereas MgH₂ required at least 30 min to reach saturation. It is evident that the incorporation of Mo markedly promoted the hydrogen adsorption rate of MgH₂.

3.3. Evolution of Flake-like Molybdenum in Cyclic Processes and Its Catalytic Mechanism

XRD tests were performed to investigate the evolution of flake-like Mo in the process of hydrogen absorption and desorption. The results are shown in Figure 4. As can be seen in Figure 4a, the phases of the MgH₂-7wt%Mo sample after ball milling were primarily MgH₂ and Mo, indicating that no chemical reaction occurred during ball milling. In the dehydrogenated sample, the MgH₂ was all converted to Mg and the catalyst Mo was stable. After hydrogenation, Mg was converted to MgH₂ and Mo remained unchanged. The presence of a small amount of Mg was observed in the rehydrogenated sample, which may have been due to the incomplete reaction of Mg during the uptake process. Furthermore, the presence of a small amount of MgO could also be observed in all three states. The microscopic morphology of the samples was observed using TEM tests. From Figure 4b it can be seen that the size of the ball-milled MgH₂-7wt%Mo was 300–500 nm. In the SAED pattern (Figure 4c), the (200) crystal face ($d = 0.157$ nm), (110) ($d = 0.222$ nm) crystal face of Mo, and the (101) crystal face of MgH₂ ($d = 0.199$ nm) were observed. The high resolution transmission electron microscopy pattern (Figure 4d) reveals that the material phases had a lattice of 0.199 nm and 0.312 nm, corresponding to the (101) crystal face of MgH₂ and the (200) crystal face of Mo, respectively. TEM analysis shows that the distribution of the Mo catalyst in the MgH₂ matrix was relatively tight, and that the sufficient contact provided by the large area of the two-dimensional lamellar structure accelerated the diffusion of hydrogen along the interface. Based on the above discussion, the improved effect of Mo flakes on the hydrogen storage performance of MgH₂ can be attributed to the inherent catalytic activity and advantage of lamellar structure.

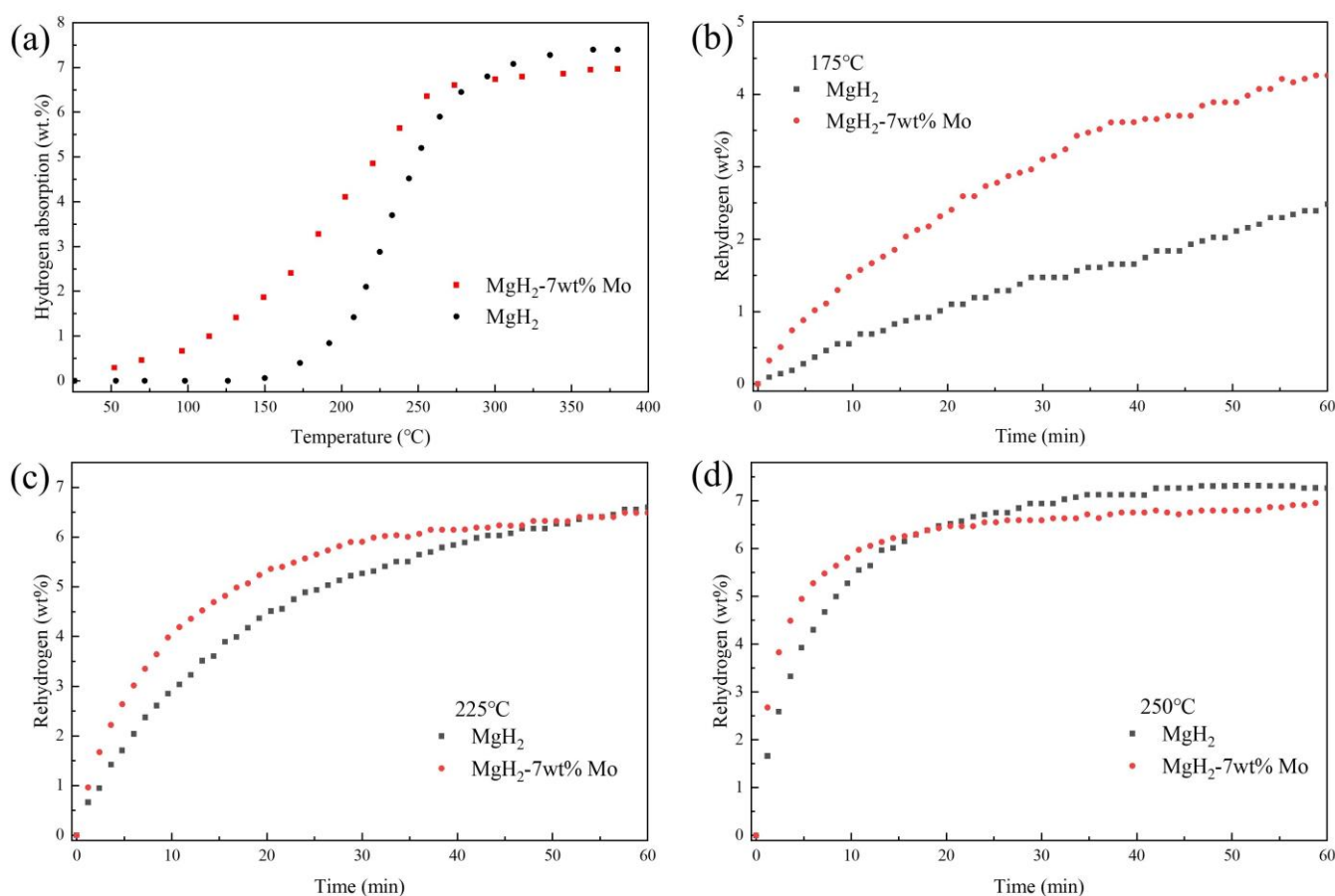


Figure 3. (a) Non-isothermal hydrogen absorption curves of MgH_2 and $\text{MgH}_2\text{-7wt\%Mo}$; comparison of isothermal hydrogenation curves of $\text{MgH}_2\text{-7wt\%Mo}$ and MgH_2 at (b) 175 °C, (c) 225 °C, and (d) 250 °C.

Cycling performance is an important indicator for assessing hydrogen storage materials. To further investigate the hydrogen storage performance of $\text{MgH}_2\text{-7wt\%Mo}$, 22 hydrogen absorption and desorption cycles were carried out at 350 °C, as shown in Figure 5a. There was no significant decline in hydrogen capacity or kinetics during the cycling. To further understand the variability in capacity, we compared the 1st and last hydrogen uptake and release curves, as shown in Figure 5b,c. In the 1st cycle, the composite released approximately 6.9 wt% of hydrogen in 20 min, and in the 22nd cycle approximately 6.8 wt% of hydrogen was released in the same time. However, it can be seen that in the initial state of the 22nd hydrogen release there was a gentle slope in the hydrogen release curve (not present in the 1st cycle), indicating a decrease in the rate of hydrogen release compared to the 1st cycle. When hydrogen adsorption rates were compared, the 1st cycle's hydrogen adsorption reached a plateau relatively quickly and rose slowly to reach 6.9 wt% of hydrogen content, whereas the 22nd cycle was only able to adsorb approximately 6.8 wt% of hydrogen. This decrease in hydrogen absorption capacity during cycling could be attributed to the formation of unreacted Mg particles in the center of the sample, a phenomenon that has been studied accordingly in other works [41]. This conjecture is consistent with the phenomenon of incompletely reacted Mg observed via XRD. Agglomeration and growth of particles can easily occur during cycling, which tends to lead to a longer diffusion path of H_2 from the outside to the inside, resulting in a decrease in kinetics and hydrogen storage capacity.

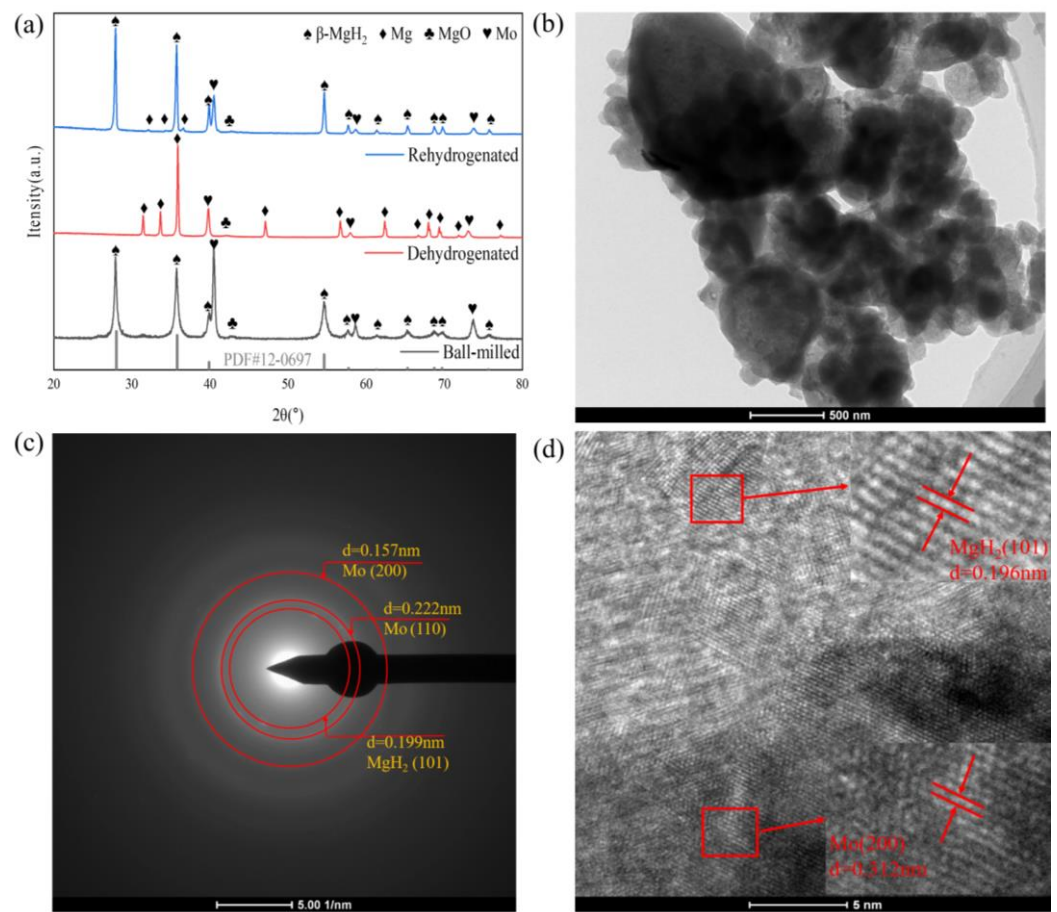


Figure 4. (a) XRD patterns of MgH₂-7wt%Mo ball-milled, dehydrogenated, and rehydrogenated; (b) TEM image; (c) SAED pattern; and (d) HRTEM image of ball-milled MgH₂-7wt%Mo.

Combining the analyses of XRD and TEM results, the physical phase changes and distribution of lamellar Mo were observed. The catalyst Mo did not react during the overall reaction and acted as stable active sites. The catalytic mechanism is shown in Figure 6. After ball milling, lamellar Mo was randomly distributed on the MgH₂ matrix. The presence of Mo can effectively promote the dissociation of H₂ molecules; the lamellar structure generated a favorable environment (a large number of contact interfaces and diffusion channels) to accelerate the diffusion of H₂ at the Mg/MgH₂ interfaces, thus significantly improving the hydrogen storage performance of MgH₂. On the other hand, lamellar Mo can effectively prevent Mg/MgH₂ particles from agglomeration and maintain the performance stability of the MgH₂-7wt%Mo composite.

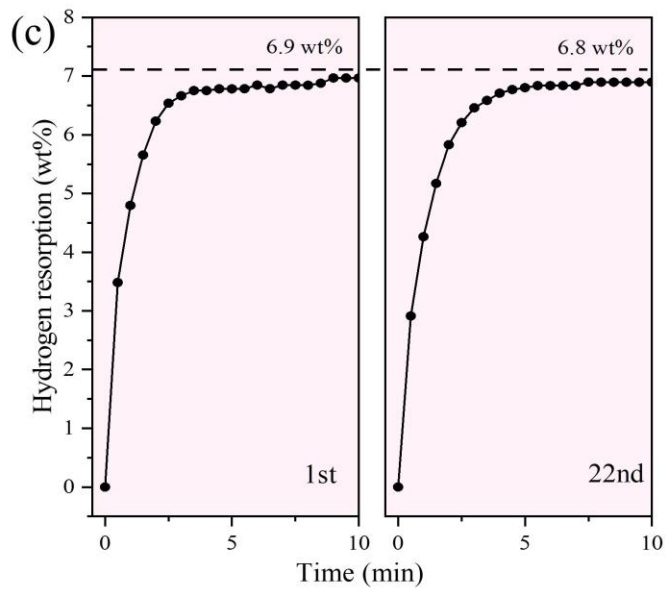
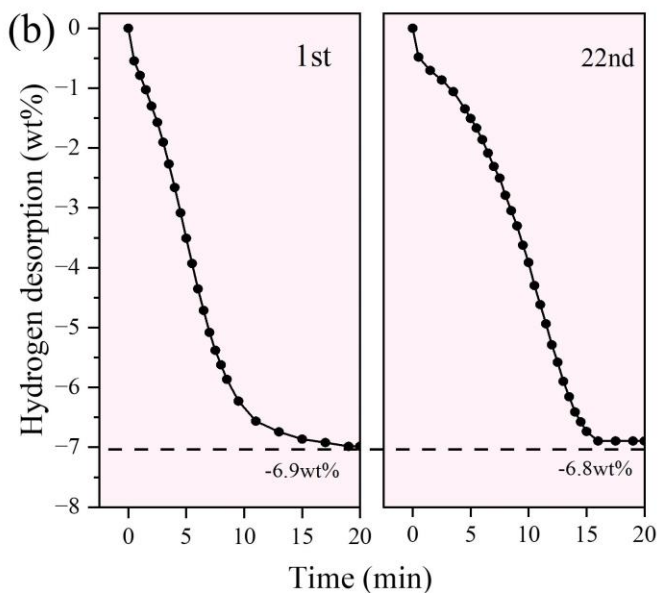
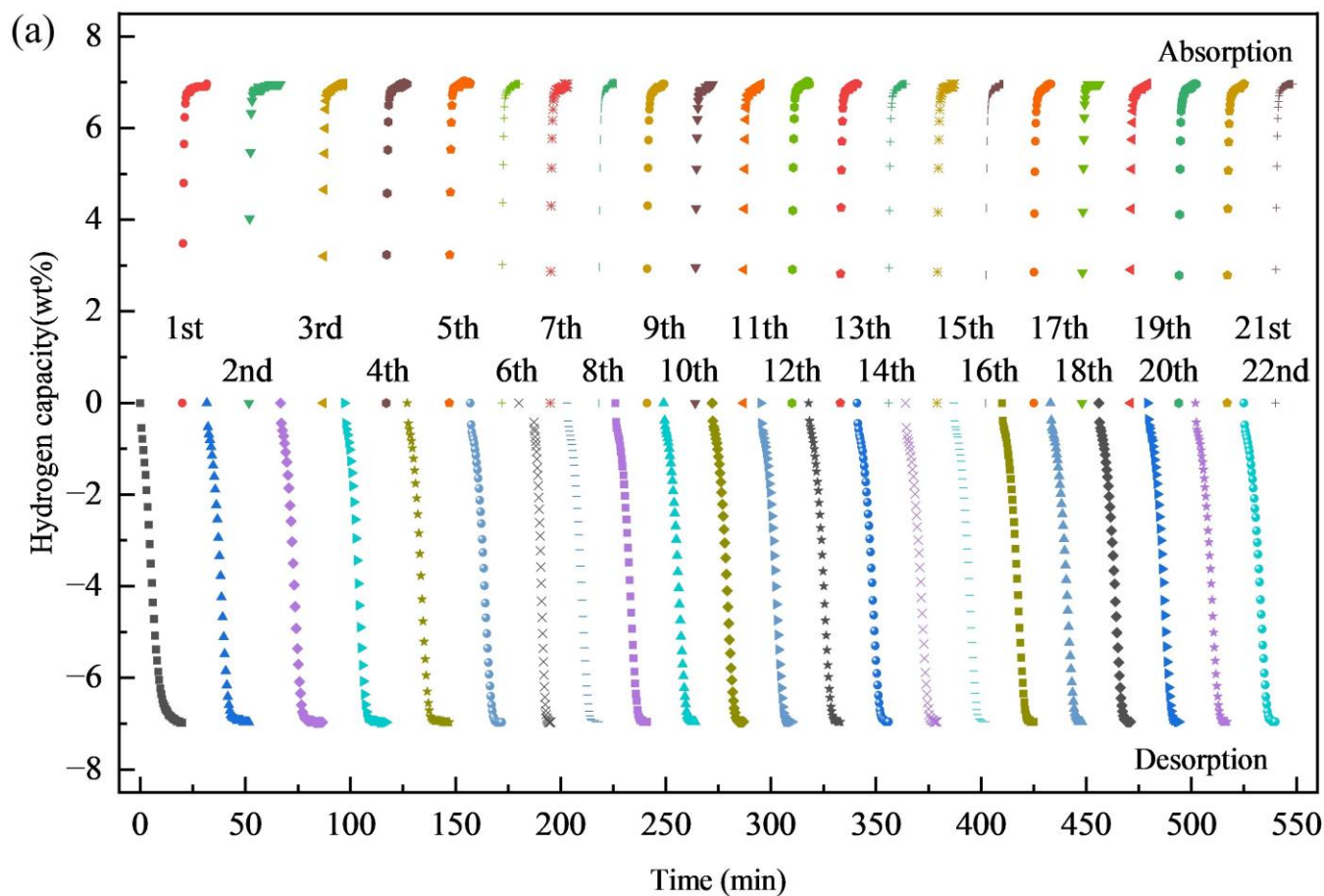


Figure 5. (a) Kinetic curves of isothermal hydrogenation (at 30 bar H₂) and dehydrogenation cycles of MgH₂-7wt%Mo composite from the 1st to the 22nd cycle at 350 °C; (b) the 1st and 22nd isothermal dehydrogenation curves of the composite at 350 °C; and (c) the 1st and 22nd isothermal hydrogen absorption curves of the composite at 350 °C.

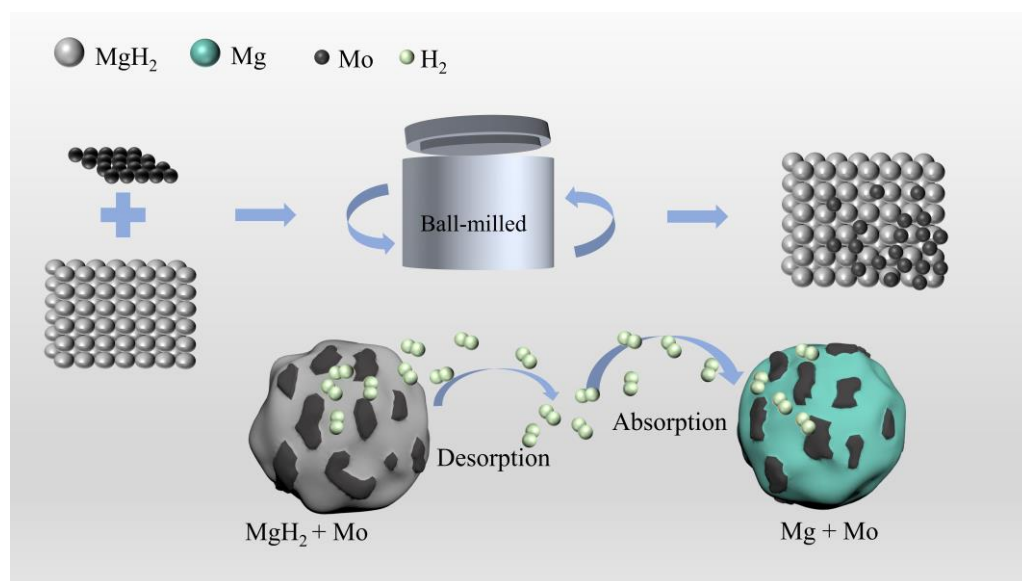


Figure 6. Schematic catalytic diagram of the MgH₂-7wt%Mo composite.

4. Conclusions

In this study, Mo flakes were successfully synthesized and adopted to improve the hydrogen storage properties of MgH₂. The MgH₂-7wt%Mo composite started desorption at 250 °C, 100 °C lower than MgH₂; when maintained at 325 °C for 20 min, 6.5 wt% hydrogen was released from the composite. During hydrogenation, the composite began to absorb hydrogen at room temperature and charged nearly 6 wt% of hydrogen in 10 min at 250 °C. Additionally, the MgH₂-7wt%Mo composite was able to maintain a high capacity of 98% after 22 hydrogenation and dehydrogenation cycles. Microstructural analysis revealed that the lamellar structure of Mo generated a favorable environment (a large number of contact interfaces and diffusion channels) to accelerate the diffusion of H₂ at the Mg/MgH₂ interfaces. Mo also remained stable during dehydrogenation and hydrogenation reactions, and served as an active catalytic union to improve the hydrogen storage properties of MgH₂.

Author Contributions: Design of experiments, data compilation, and writing—original manuscript, C.C.; writing—review and editing, H.Z. and M.S.; software, visualization, and supervision, F.W.; methods, review and editing, and supervision, L.Z. All authors have read and agreed to the published version of the manuscript.

Funding: This work was supported by the National Natural Science Foundation of China (Grant No. 51801078).

Institutional Review Board Statement: Not applicable.

Informed Consent Statement: Not applicable.

Data Availability Statement: The data presented in this study are available on request from the corresponding author.

Conflicts of Interest: The authors declare no conflict of interest.

References

1. Shao, H.; He, L.; Lin, H. Progress and Trends in Mg-based Materials for Energy Storage Research: A Review. *Energy Technol.* **2018**, *6*, 445–448. [CrossRef]
2. Jain, I.P. Hydrogen the fuel for 21st century. *Int. J. Hydrogen Energy* **2009**, *34*, 7368–7378. [CrossRef]
3. Zhang, J.; Yan, S.; Qu, H. Recent progress in magnesium hydride modified through catalysis and nanoconfinement. *Int. J. Hydrogen Energy* **2018**, *43*, 1545–1565. [CrossRef]
4. Zhang, X.; Liu, Y.; Zhang, X. Empowering hydrogen storage performance of MgH₂ by nanoengineering and nanocatalysis. *Mater. Today Nano* **2020**, *9*, 10064. [CrossRef]

5. Zhang, J.; Yan, S.; Qu, H. Stress/strain effects on thermodynamic properties of magnesium hydride: A brief review. *Int. J. Hydrogen Energy* **2017**, *42*, 16603–16610. [[CrossRef](#)]
6. Kim, C.K. A review on design strategies for metal hydrides with enhanced reaction thermodynamics for hydrogen storage applications. *Int. J. Energy Res.* **2018**, *42*, 1455–1468. [[CrossRef](#)]
7. Sadhasivam, T.; Kim, H.-T.; Jung, S.; Roh, S.-H.; Park, J.-H.; Jung, H.-Y. Dimensional effects of nanostructured Mg/MgH₂ for hydrogen storage applications: A review. *Renew. Sust. Energy Rev.* **2017**, *72*, 523–534. [[CrossRef](#)]
8. El-Eskandarany, M.S. Recent developments in the fabrication, characterization and implementation of MgH₂-based solid-hydrogen materials in the Kuwait Institute for Scientific Research. *RSC Adv.* **2019**, *9*, 9907–9930. [[CrossRef](#)]
9. Tian, M.; Shang, C.X. Nano-structured MgH₂ catalyzed by TiC nanoparticles for hydrogen storage. *J. Chem. Technol. Biotechnol.* **2011**, *8*, 69–74. [[CrossRef](#)]
10. Bhatnagar, A.; Johnson, J.K.; Shaz, M.A.; Srivastava, O.N. H₂ as a dynamic additive for improving the de/rehydrogenation properties of MgH₂: A combined experimental and theoretical mechanistic investigation. *J. Phys. Chem. C* **2018**, *122*, 21248–21261. [[CrossRef](#)]
11. Zhang, L.; Ji, L.; Yao, Z.; Yan, N.; Sun, Z.; Yang, X.; Zhu, X.; Hu, S.; Chen, L. Facile synthesized Fe nanosheets as superior active catalyst for hydrogen storage in MgH₂. *Int. J. Hydrogen Energy* **2019**, *44*, 21955–21964. [[CrossRef](#)]
12. Jain, I.P.; Lal, C.; Jain, A. Hydrogen storage in Mg: A most promising material. *Int. J. Hydrogen Energy* **2010**, *35*, 5133–5144. [[CrossRef](#)]
13. Kumar, S.; Ankur, J.; Yamaguchi, J.S. Surface modification of MgH₂ by ZrCl₄ to tailor the reversible hydrogen storage performance. *Int. J. Hydrogen Energy* **2017**, *42*, 6152–6159. [[CrossRef](#)]
14. Shevlin, S.A.; Guo, Z.X. MgH₂ dehydrogenation thermodynamics: Nanostructuring and transition metal doping. *J. Phys. Chem. C* **2013**, *117*, 10883–10891. [[CrossRef](#)]
15. Ouyang, L.Z.; Cao, Z.J.; Wang, H. Enhanced dehydriding thermodynamics and kinetics in Mg(In)–MgF₂ composite directly synthesized by plasma milling. *J. Alloys Compd.* **2014**, *586*, 113–117. [[CrossRef](#)]
16. Leiva, D.R.; Jorge, A.M.; Ishikawa, T.T.; Huot, J.; Fruchart, D.; Miraglia, S.; Kiminami, C.S.; Botta, W.J. Nanoscale Grain Refinement and H-Sorption Properties of MgH₂ Processed by High-Pressure Torsion and Other Mechanical Routes. *Adv. Eng. Mater.* **2010**, *12*, 786–792. [[CrossRef](#)]
17. Alsabawi, K.; Gray, E.M.; Webb, C.J. The effect of ball-milling gas environment on the sorption kinetics of MgH₂ with/without additives for hydrogen storage. *Int. J. Hydrogen Energy* **2019**, *44*, 2976–2980. [[CrossRef](#)]
18. Zhang, M.; Xiao, X.; Wang, X.; Chen, M.; Lu, Y.; Liu, M.; Chen, L. Excellent catalysis of TiO₂ nanosheets with high-surface-energy {001} facets on the hydrogen storage properties of MgH₂. *Nanoscale* **2019**, *11*, 7465–7473. [[CrossRef](#)]
19. Lu, Z.Y.; Yu, H.J.; Lu, X.; Song, M.C.; Wu, F.Y.; Zheng, J.G.; Yuan, Z.F.; Zhang, L.T. Two-dimensional vanadium nanosheets as a remarkably effective catalyst for hydrogen storage in MgH₂. *Rare Met.* **2021**, *40*, 3195–3204. [[CrossRef](#)]
20. Yan, N.Y.; Lu, X.; Lu, Z.Y.; Yu, H.J.; Wu, F.Y.; Zheng, J.G.; Wang, X.Z.; Zhang, L.T. Enhanced hydrogen storage properties of Mg by the synergistic effect of grain refinement and NiTiO₃ nanoparticles. *J. Magnes. Alloys* **2022**, *10*, 3542–3552. [[CrossRef](#)]
21. Ismail, M. Effect of LaCl₃ addition on the hydrogen storage properties of MgH₂. *Energy* **2015**, *79*, 177–182. [[CrossRef](#)]
22. Song, M.C.; Zhang, L.T.; Zheng, J.G.; Yu, Z.D.; Wang, S.N. Constructing graphene nanosheets supported FeOOH nanodots for hydrogen storage of MgH₂. *Int. J. Min. Met. Mater.* **2022**, *29*, 1464–1473. [[CrossRef](#)]
23. Soni, P.K.; Bhatnagar, A.; Shaz, M.A.; Srivastava, O.N. Effect of graphene templated fluorides of Ce and La on the de/rehydrogenation behavior of MgH₂. *Int. J. Hydrogen Energy* **2017**, *42*, 20026–20035. [[CrossRef](#)]
24. Chen, G.; Zhang, Y.; Chen, J. Enhancing hydrogen storage performances of MgH₂ by Ni nano-particles over mesoporous carbon CMK-3. *Nanotechnology* **2018**, *29*, 265705. [[CrossRef](#)] [[PubMed](#)]
25. Lu, Y.; Kim, H.; Sakaki, K.; Hayashi, S.; Jimura, K.; Asano, K. Destabilizing the Dehydrogenation Thermodynamics of Magnesium Hydride by Utilizing the Immiscibility of Mn with Mg. *Inorg. Chem.* **2019**, *58*, 14600–14607. [[CrossRef](#)]
26. Ma, Z.; Zou, J.; Khan, D.; Zhu, W.; Hu, C.; Zeng, X.; Ding, W. Preparation and hydrogen storage properties of MgH₂-trimesic acid-TM MOF (TM = Co, Fe) composites. *J. Mater. Sci. Technol.* **2019**, *35*, 2132–2143. [[CrossRef](#)]
27. Wang, Y.; Ding, Z.; Li, X.; Ren, S.; Zhou, S.; Zhang, H.; Han, S. Improved hydrogen storage properties of MgH₂ by nickel@nitrogen-doped carbon spheres. *Dalton Trans.* **2020**, *20*, 3495–3502. [[CrossRef](#)] [[PubMed](#)]
28. Peng, D.; Ding, Z.; Fu, Y. Enhanced H₂ sorption performance of magnesium hydride with hard-carbon-sphere-wrapped nickel. *RSC Adv.* **2018**, *8*, 28787–28796. [[CrossRef](#)]
29. Lu, X.; Zhang, L.T.; Yu, H.J.; Lu, Z.Y.; He, J.H.; Zheng, J.G.; Wu, F.Y.; Chen, L.X. Achieving superior hydrogen storage properties of MgH₂ by the effect of TiFe and carbon nanotubes. *Chem. Eng. J.* **2021**, *422*, 130101. [[CrossRef](#)]
30. Tarasov, B.P.; Mozzhukhin, S.A.; Arbutov, A.A.; Volodin, A.A.; Fokina, E.E.; Fursikov, P.V.; Lototsky, M.V.; Yartys, V.A. Features of the Hydrogenation of Magnesium with a Ni-Graphene Coating. *Russ. J. Phys. Chem. A* **2020**, *94*, 996–1001. [[CrossRef](#)]
31. Zhang, L.; Yu, H.; Lu, Z.; Zhao, C.; Zheng, J.; Wei, T.; Wu, F.; Xiao, B. The effect of different Co phase structure (FCC/HCP) on the catalytic action towards the hydrogen storage performance of MgH₂. *Chin. J. Chem. Eng.* **2022**, *43*, 343–352. [[CrossRef](#)]
32. Wang, K.; Deng, Q. Constructing Core-Shell Co@N-Rich Carbon Additives Toward Enhanced Hydrogen Storage Performance of Magnesium Hydride. *Front. Chem.* **2020**, *8*, 233. [[CrossRef](#)]
33. Ding, X.; Ding, H.; Song, Y. Activity-Tuning of Supported Co–Ni Nanocatalysts via Composition and Morphology for Hydrogen Storage in MgH₂. *Front. Chem.* **2020**, *7*, 937. [[CrossRef](#)] [[PubMed](#)]

34. Ji, L.; Zhang, L.; Yang, X.; Zhu, X.; Chen, L. Remarkably improved hydrogen storage performance of MgH₂ by the synergetic effect of FeNi/rGO nanocomposite. *Dalton Trans.* **2020**, *49*, 4146–4154. [[CrossRef](#)] [[PubMed](#)]
35. Schimmel, H.G.; Huot, J.; Chapon, L.C.; Tichelaar, F.D.; Mulder, F.M. Hydrogen Cycling of Niobium and Vanadium Catalyzed Nanostructured Magnesium. *J. Am. Chem. Soc.* **2005**, *127*, 14348–14354. [[CrossRef](#)]
36. Yan, C.H.; Zhang, H.Y.; Wu, F.Y.; Ze, S.U.; Zheng, J.G.; Zhang, L.T.; Chen, L.X. Mn nanoparticles enhanced dehydrogenation and hydrogenation kinetics of MgH₂ for hydrogen storage. *Trans. Nonferrous Met. Soc. China* **2021**, *31*, 3469–3477.
37. Jia, Y.; Han, S.; Zhang, W.; Zhao, X.; Sun, P.; Liu, Y.; Shi, H.; Wang, J. Hydrogen absorption and desorption kinetics of MgH₂ catalyzed by MoS₂ and MoO₂. *Int. J. Hydrogen Energy* **2013**, *38*, 2352–2356. [[CrossRef](#)]
38. Chen, M.; Pu, Y.; Li, Z.; Huang, G.; Liu, X.; Lu, Y.; Tang, W.; Xu, L.; Liu, S.; Yu, R.; et al. Synergy between metallic components of MoNi alloy for catalyzing highly efficient hydrogen storage of MgH₂. *Nano Res.* **2020**, *13*, 2063–2071. [[CrossRef](#)]
39. Xia, G.; Leng, H.; Xu, N.; Li, Z.; Wu, Z.; Du, J.; Yu, X. Enhanced hydrogen storage properties of LiBH₄-MgH₂ composite by the catalytic effect of MoCl₃. *Int. J. Hydrogen Energy* **2011**, *36*, 7128–7135. [[CrossRef](#)]
40. Wang, J.; Du, Y.; Sun, L.; Li, X. Effects of F and Cl on the stability of MgH₂. *Int. J. Hydrogen Energy* **2014**, *39*, 877–883. [[CrossRef](#)]
41. Song, M.; Zhang, L.; Yao, Z.; Zheng, J.; Shang, D.; Chen, L.; Li, H. Unraveling the degradation mechanism for the hydrogen storage property of Fe nanocatalyst-modified MgH₂. *Inorg. Chem. Front.* **2022**, *9*, 3874. [[CrossRef](#)]

Disclaimer/Publisher’s Note: The statements, opinions and data contained in all publications are solely those of the individual author(s) and contributor(s) and not of MDPI and/or the editor(s). MDPI and/or the editor(s) disclaim responsibility for any injury to people or property resulting from any ideas, methods, instructions or products referred to in the content.